Biochemistry and Biophysics Reports 39 (2024) 101758

Contents lists available at ScienceDirect

Biochemistry and Biophysics Reports

journal homepage: www.elsevier.com/locate/bbrep

In silico and ADMET molecular analysis targeted to discover novel anti-inflammatory drug candidates as COX-2 inhibitors from specific metabolites of *Diospyros batokana* (Ebenaceae)

Bitwell Chibuye [a,b,c,*], Indra Sen Singh [b], Luke Chimuka [c], Kenneth Kakoma Maseka [b]

[a] Department of Chemistry, Mukuba University, PO Box 20382, Itimpi Campus, Kitwe, Zambia
[b] Department of Chemistry, School of Mathematics and Natural Sciences, The Copperbelt University, PO Box 21692, Kitwe, Zambia
[c] Molecular Sciences Institute, School of Chemistry, University of Witwatersrand, Johannesburg, South Africa

ARTICLE INFO

Keywords:
Diospyros batokana (Ebenaceae)
In silico molecular docking
Anti-inflammatory
Drug likeness
Bioavailability radar
Physicochemical properties

ABSTRACT

Diospyros batokana (Ebenaceae) is a valuable medicinal plant that grows in the wild in Zambia. The aqua crude plant extract is valuable in treating oxidative stress and microbes-related diseases. In this study, bioactive metabolites from the leaf of the plant were tentatively identified using ultra-high-pressure liquid chromatography tandem high-resolution mass spectrometry (UHPLC-HRMS). Raw LCMS data were processed using MZmine3.6. Pyrenophorol, N-[1-(diethylamino)-3-morpholin-4-ylpropan-2-yl]-2,2-diphenylacetamide, losartan, and isoarthonin, (2E,4E)-N-[2-(4-hydroxyphenyl)ethyl]dodeca-2,4-dienamide were among the many metabolites identified from the plant studied using LCMS-MZmine 3.6. Furthermore, in silico anti-inflammatory molecular docking was applied to the five (5) metabolites with the aim of predicting the ability of the metabolites to inhibit the COX-2 enzyme. The docking simulation for the five metabolites was executed using the Auto-dock tools. The lowest binding energy of the complexes was visualized using Discovery Studio, 2021 Client l molecular viewer. Pyrenophorol, (N-[1-(diethylamino)-3-morpholin-4-ylpropan-2-yl] −2,2-diphenylacetamide) and losartan were found to provide the lowest binding energy to COX-2 compared to the standard anti-inflammatory drug, diclofenac. Furthermore, binding affinities, inhibition constants, and ligand efficiencies demonstrated that pyrenophorol, N-[1-(diethylamino)-3-morpholin-4-ylpropan-2-yl]-2,2-diphenylacetamide, losartan, isoarthonin and (2E,4E)-N-[2-(4-hydroxyphenyl)ethyl]dodeca-2,4-dienamide could be useful as anti-inflammatory drug candidates supporting the traditional uses of *D. batokana*. However, the bioavailability radar and physicochemical properties only predict losartan, pyrenophorol, and (2E,4E)-N-[2-(4-hydroxyphenyl)ethyl]dodeca-2,4-dienamide to be bioavailable and suitable drug candidates. In silico and ADMET analysis, shows that the five metabolites could be used as anti-inflammatory drugs comparable to the standard drugs, diclofenac and ibuprofen. However, in vitro and in vivo studies are needed to further support our findings.

1. Introduction

The natural immune system uses inflammation to defend itself against harmful stimuli or pathogens. However, inflammation can also be reflected as a symptom of various diseases. It is a multifaceted response to cell injury, infection, or exposure to toxins, showing both short-lived and chronic forms of inflammation [1]. The immune cells' excessive production of inflammatory cytokines and targets by immune cells plays a crucial role in the regulation of these inflammatory reactions. In addition, inflammation induced by oxidative stress can contribute to chronic conditions such as diabetes and cancer [2]. Non-steroidal medicines (NSMs) are commonly prescribed to address inflammation due to their analgesic properties. Aspirin, a classic drug with a long history of use, is one such example [3]. Similarly, various NSMs such as diclofenac, ibuprofen, celecoxib, and others have been developed and used in conjunction with aspirin. The mechanism of operation of these medications involves inhibiting the cyclooxygenase enzyme (COX), which mediates the biological conversion of arachidonic acid into inflammatory prostaglandins [4,5].

Among the three COX isoforms (COX1, COX 2, and COX 3), COX 2 plays a crucial role in various diseases, including respiratory problems, rheumatoid arthritis, cancer, neuropsychiatric disorders, depressive

* Corresponding author. Department of Chemistry, Mukuba University, PO Box 20382, Itimpi Campus, Kitwe, Zambia.
E-mail address: bitwellchibuye@gmail.com (B. Chibuye).

https://doi.org/10.1016/j.bbrep.2024.101758
Received 25 April 2024; Received in revised form 10 June 2024; Accepted 14 June 2024
Available online 13 July 2024

disorders, osteoarthritis, and respiratory problems [6]. The most commonly used treatment for inflammation involves non-steroidal COX 2 inhibitors. However, this approach has a drawback as it can lead to side effects such as cardiovascular complications, including stroke, blood clots, and heart attacks. Consequently, there is an urgent need to discover and develop new COX-2 inhibitors that are specific and have minimal or no side effects [7,8]. Cyclooxygenases (COX 1, COX 2, and COX 3) are responsible for the production of prostaglandins (PGs), crucial molecules that mediate inflammatory processes [9,10]. In inflammatory tissues, COX 2 is the primary determinant of prostaglandin synthesis levels, a molecule actively involved in various physiological processes, including generating inflammatory responses [11].

Many medicinal plants contain abundant anti-inflammatory compounds [12]. Traditionally, plants have been used in medicine to alleviate inflammation. However, there is a significant gap in research supporting their anti-inflammatory properties, as these plants have yet to undergo thorough pharmacological or toxicological investigations to validate their ant-inflammatory bioactivity. One such plant, Diospyros batokana (Ebenaceae), is traditionally used in Zambia to treat various degenerative diseases [13].

In pharmaceutical development, computational models such as absorption, distribution, metabolism, excretion, and toxicity (ADMET) are essential for quickly evaluating important properties of potential drug candidates. This initial screening helps prioritize compounds for more thorough investigations in vitro and in vivo [14–17]. In this study, we analyzed the ADMET properties of selected bioactive phytochemicals compared to a reference drug. The notable findings from the ADMET assessment underscore the importance of further exploration of these molecules through comprehensive in vitro and in vivo analyzes.

In medicinal chemistry, where the synthesis of new compounds involves manipulating the lead moiety to make highly active compounds with minimal steric effects, drug design plays a vital role. A significant advancement in the drug design process was the advent of the in silico approach to predict a molecule's therapeutic efficacy [18]. Due to the lack of research on the anti-inflammatory properties of metabolites from *D. batokana* and interesting findings from a previous study on *D. batokana*, which included phytochemical screening, total polyphenolic content, and antioxidant potential determinations, the authors were prompted to explore new inhibitors of COX 2 from these identified metabolites [13]. Therefore, five ligands were selected for in silico molecular analysis to discover new COX-2 inhibitors and performed ADMET analysis of these ligands, with diclofenac and ibuprofen as references in this study.

This study encompasses in silico anti-inflammatory molecular docking analysis, physicochemical property assessment, and drug-likeness evaluation of five metabolites from the medicinal plant D. batokana. The current research is based solely on in silico models and predictions. Nonetheless, the promising results obtained strongly suggest the need for experimental validation through in vitro or in vivo studies to confirm the anti-inflammatory activities. Therefore, future research should include in vitro or in vivo studies to further investigate the anti-inflammatory effects.

2. Materials and methods

2.1. Identification of ligands using MZmine 3.6

For bioactive metabolite annotation, the MS2 Bruker data file from Chibuye et al. (2023) [13] was used to identify metabolites using the molecular networking tool MZmine 3.6, through two standard workflows as depicted below [19–21]:

Workflow 1: Data conversion to a mzML file

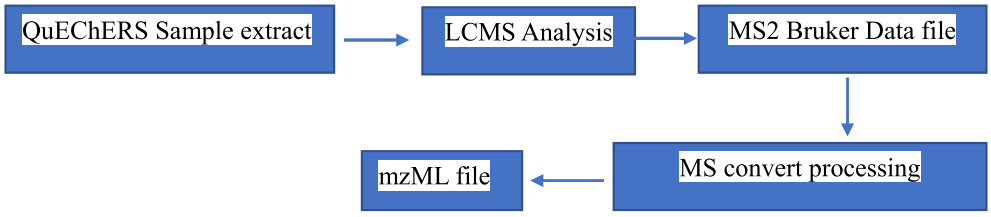

Workflow 2: MZmine 3.6 standard workflow

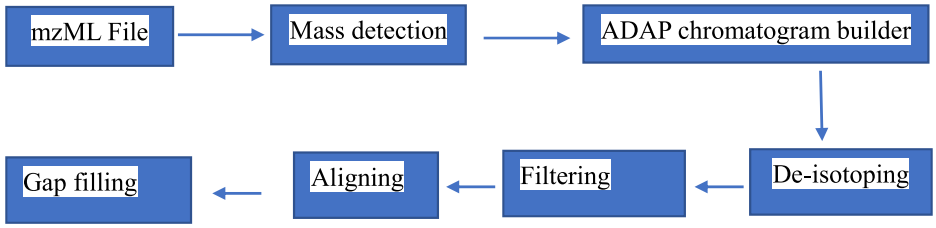

After completing the above workflows in Section 2.1 and exporting MGF and csv files, workflow for annotation, the feature list method was followed. This step included selecting annotation followed by the search spectra option and then finally choosing spectral library search from an already imported library from the feature list method; in this case, we used the MoNA library. Finally, the spectral library search option was selected to annotate metabolites from the MoNa library. Table 1 shows fifty-seven (57) metabolites tentatively identified by LCMS/MS - MZmine 3.6. Some features such as retention time, precursor *m/z*, MS2 fragmentation, and cosine similarity are also shown in Table 1. The five metabolites of interest can easily be identified in Table 1.

2.2. Preparation of ligands

Five (5) ligand metabolites (Fig. 1) were selected from the metabolites identified in D. batokana in Table 1. The metabolites were only tentatively identified using mass spectrometry data and molecular networking tools. In future studies, it may also be worthwhile to apply techniques such as NMR to concretize the characterization of these

Table 1
Identification based on MZmine 3.6 of metabolites from the crude extract of the stem bark of *Diospyros batokana, Ebenaceae* by UHPLC−ESI-MS/MS in the negative ion mode. Base peaks are indicated in bold.

ID	RT	Adduct [M − H]−	Exact Mass	MS2	Tentative Compound	Formula	Cosine similarity
1	1.76	409.0442	410.3510	**96.95**, 132.03, 173.03, 251.08, 409.07	Vanillic acid + O-sulfonateHex	$C_{14}H_{18}O_{12}S$	0.868
2	1.87	[M+HCOO]- 399.0930	354.3110	85.02, 129.03, 159.02, **191.05**	Coumarin base + 1O, 1MeO, O-Hex	$C_{16}H_{18}O_9$	0.751
3	1.89	223.0612	224.0685	75.01, 85.02, **125.02**, 147.02, 162.04, 205.03	Trinexapac,	$C_{11}H_{12}O_5$	0.901
4	1.89	192.1030	193.1103	72.99, 87.00, 113.02, 174.04, **192.05**	N,N-Diethyl-4-hydroxybenzamide	$C_{11}H_{15}NO_2$	0.759
5	1.91	408.3500		**90.95**, 132.35, 154.04, 191.05, 311.08	Benzylglucosinolate	$C_{14}H_{19}NO_9S_2$	0.951
6	2.00	188.0717		80.91, **142.05**	Indolepropionic acid	$C_{11}H_{11}NO_2$	0.888
7	2.09	345.1344		124.01, 152.02, 192.55, 233.06, 255.03, 330.04, **345.06**	isotaxiresinol	$C_{19}H_{22}O_6$	0.780
8	2.20	345.0616	346.0689	109.02, 124.01, 139.04, 191.04, 255.04, 286.06, 230.04, **345.07**	Limocitrin	$C_{17}H_{14}O_8$	0.808
9	2.44	345.0616	346.0689	95.05, 138.02, 166.02, 191.04, 255.04, 286.06, 230.04, 303.09, 330.04, **345.07**	Limocitrin (isomer)	$C_{17}H_{14}O_8$	0.787
10	2.46	345.0000	346.1780	85.02, 124.01, 180.00, 225.03, 255.04, 301.08, 330.05, **345.07**	Gibberellin A24	$C_{20}H_{26}O_5$	0.756
11	2.71	191.0197	192.0270	**87.00**, 99.05, 111.00	Citric acid	$C_6H_8O_7$	0.983
12	2.72	191.0561		**87.00**, 111.00, 191.05	Quinic acid	$C_7H_{12}O_6$	0.900
13	2.78	191.0350	192.0270	87.00, **111.00,** 129.01	Citric acid	$C_6H_8O_7$	0.983
14	3.52	345.1344		138.02, 152.00, 191.05, 210.00, 225.03, 250.04, 286.99, 330.05, **345.07**	Isotaxiresinol (isomer)	$C_{19}H_{22}O_6$	0.768
15	3.90	169.0220	170.0210	79.01, 81.03, 107.01, **125.02**	Gallic acid	$C_7H_6O_5$	0.946
16	3.96	169.0142	170.0215	79.01, 81.03, 95.01, 108.02, **125.02**	Gallic acid	$C_7H_6O_5$	0.972
17	3.96	169.0142	170.0210	79.01, 81.03, 97.02, 107.00, **125.02**	Gallic acid	$C_7H_6O_5$	0.968
18	4.07	169.0000	170.0215	81.03, 97.03, 107.02, **125.02**	Gallate	$C_7H_6O_5$	0.968
19	4.10	302.1299	303.3650	107.01, 125.02, 136.98, **169.01**	Evodiamine	$C_{19}H_{17}N_3O$	0.951
20	4.16	448.3068	449.3141	136.99, 173.04, 259.13, 311.16, **403.18**	Glycochenodeoxycholate	$C_{26}H_{43}NO_5$	0.773
21	4.16	315.1966		107.01, 125.02, **169.01**, 269.09	(1S,4aS,5R)-5-[2-(furan-3-yl)ethyl]-1,4a-dimethyl-6-methylidene-3,4,5,7,8,8a-hexahydro-2H-naphthalene-1-carboxylic acid	$C_{20}H_{28}O_3$	0.947
22	4.17			89.02, 113.02, **149.04**, 179.02, 203.03, 371.09	Glucoraphanin	$C_{12}H_{23}NO_{10}S_3$	0.707
23	4.27	[M+HCOO]- 461.4254	416.4230	89.02, 139.07, 169.01, 225.11, **255.11**, 293.08, 231.05	Phenylethanol + Hex-Pen	$C_{19}H_{28}O_{10}$	0.711
24	4.27	301.2173		71.01, 107.01, 125.01, **169.01**, 197.04, 209.95	7-ethenyl-1,4a,7-trimethyl-3,4,6,8,8a,9,10,10a-octahydro-2H-phenanthrene-1-carboxylic acid	$C_{20}H_{30}O_2$	0.898
25	4.27	314.2126		81.03, 109.03, 123.04, 137.02, 179.03, **193.00**, 235.01	(2E,4E)-N-[2-(4-hydroxyphenyl)ethyl]dodeca-2,4-dienamide	$C_{20}H_{29}NO_2$	0.957
26	4.30	[M+HCOO]- 450.2345		135.07, 179.04, 225.13, 293.07, **405.20**	HexCer 10:1; 2O/3:0	$C_{19}H_{35}NO_8$	0.754
27	4.35	507.1508		80.96, 125.02, 169.01, 301.08, 336.12, 361.02, 461.39, **507.12**	Scutellarioside II	$C_{24}H_{28}O_{12}$	0.802
28	4.35	509.2550	510.2620	80.96, 125.02, 169.01, 301.08, 336.12, 361.02, 461.39, **507.12**	2-[(2R,4aS,8S,8aS)-8-[2-[(4aS,7R,8aR)-7-(1-carboxyethenyl)-1-hydroxy-4a-methyl-2-oxo-6,7,8,8a-tetrahydro-5H-naphthalen-1-yl]ethyl]-4a-methyl-7-oxo-1,2,3,4,8,8a-hexahydronaphthalen-2-yl]prop-2-enoic acid	$C_{30}H_{38}O_7$	0.865
29	4.39	455.2550	424.2360	101.02, 149.04, 192.05, 221.05, 267.03, 311.11, 382.11, **409.16**	Isoarthonin	$C_{25}H_{32}N_2O_4$	0.979
30	4.42	450.0568	451.0641	89.02, 113.02, 204.00, 279.10, 405.20, **451.20**	Glucoalyssin	$C_{13}H_{25}NO_{10}S_3$	0.842
31	4.58	358.27		93.03, 193.03, **173.04**, 211.03, 239.05	sinigrin	$C_{10}H_{17}NO_9S_2$	0.820
32	4.86	305.1394		101.05, 155.10, 175.05, 187.01, 201.10, **219.12**	(9a-hydroxy-3,8a-dimethyl-5-methylidene-2-oxo-4,4a,6,7,8,9-hexahydrobenzo[f] [1]benzofuran-8-yl) acetate	$C_{17}H_{22}O_5$	0.778
33	4.87	153.0190	154.0270	79.95, **109.02**	Dihydroxybenzoate	$C_7H_6O_4$	0.923

(*continued on next page*)

Table 1 (*continued*)

ID	RT	Adduct [M − H]−	Exact Mass	MS2	Tentative Compound	Formula	Cosine similarity
34	4.99	421.1549	422.1622	97.05, 125.02, 213.14, 241.06, 267.15, 375.14, **421.23**	Losartan	$C_{22}H_{23}ClN_6O$	0.992
35	5.04	449.4800		89.02, 154.00, **179.05**, 208.04, 296.05, 335.03, 403.18	[(2E,6E,10E)-3,7,11,15-tetramethylhexadeca-2,6,10,14-tetraenyl] hydrogen phosphate	$C_{20}H_{36}O_7P_2$	0.717
36	5.08	477.4300		125.02, **169.01**, 327.05, 433.23, 479.10	isorhamnetin-3-O-glucoside	$C_{22}H_{22}O_{12}$	0.866
37	5.17	495.1636		125.02, 139.03, **169.00**, 241.04, 457.06	(2R,3S,4S,5R,6R)-2-[[(2R,3R,4R)-3,4-dihydroxy-5-(hydroxymethyl)oxolan-2-yl]oxymethyl]-6-[4-(4-hydroxyphenyl)butan-2-yloxy]oxane-3,4,5-triol	$C_{21}H_{32}O_{11}$	0.756
38	5.67	[M+HCOO]- 493.2293	448.5090	113.01, **213.14**, 253.08, 316.16	Pentose-Hexose + $C_{10}H_{17}$	$C_{21}H_{36}O_{10}$	0.809
39	5.82	[M+FA-H]- 509.0930	464.0950	101.02, 163.05, 205.06, 265.08, **462.22**	3,5,7-trihydroxy-2-[4-hydroxy-3-[(2S,3R,4S,5S,6R)-3,4,5-trihydroxy-6-(hydroxymethyl)oxan-2-yl]oxyphenyl]chromen-4-one	$C_{21}H_{20}O_{12}$	0.838
40	5.93	549.0886		101.02, 234.00, 309.04, 403.25, **505.32**	Quercetin 3-O-malonylglucoside	$C_{24}H_{22}O_{15}$	0.801
41	6.20	447.05		**125.02**, 161.01, 287.0523	Glucobrassicin	$C_{16}H_{20}N_2O_9S_2$	0.772
42	6.39	332.9807		107.02, 135.03, **253.07**, 297.12	6-chloro-4,5,7-trihydroxy-9,10-dioxoanthracene-2-carboxylic acid	$C_{15}H_7ClO_7$	0.755
43	6.43	533.3499		101.02, 207.02, 245.16, 294.02, 327.05, **489.25**	Asiatic acid	$C_{30}H_{48}O_5$	0.890
44	6.67	441.0846		137.00, 339.18, **439.35**	Catechin gallate	$C_{22}H_{18}O_{10}$	0.937
45	6.68	246.9918		83.00, 95.04, 107.01, 123.04, 150.99, **167.02**, 203.02	5-Methoxysalicylic acid sulfate	$C_8H_8O_7S$	0.855
46	6.97	329.0667	330.0740	99.07, 153.09, 171.09, 229.13, 269.20, 311.10, **329.22**	Tricin	$C_{17}H_{14}O_7$	0.925
47	7.00	441.0846		173.03, 229.05, 309.17, **439.35**	Catechin gallate	$C_{22}H_{18}O_{10}$	0.880
48	7.02	509.2545		85.02, 219.09, 257.04, 301.20, **465.27**	2-[(2R,4aS,8S,8aS)-8-[2-[(4aS,7R,8aR)-7-(1-carboxyethenyl)-1-hydroxy-4a-methyl-2-oxo-6,7,8,8a-tetrahydro-5H-naphthalen-1-yl]ethyl]-4a-methyl-7-oxo-1,2,3,4,8,8a-hexahydronaphthalen-2-yl]prop-2-enoic acid	$C_{30}H_{38}O_7$	0.861
49	7.04	329.0667	330.0740	90.19, 155.10, 171.10, 229.13, 201.10, 293.20, 311.21, **329.22**	Tricin (isomer)	$C_{17}H_{14}O_7$	0.927
50	7.05	[M+FA-H]- 487.2030	442.2050	153.01, 199.05, 265.12, **439.34**	3-Hydroxy-3-(hydroxymethyl)-4-methylpentyl 6-O-[(2S,3R,4R)-3,4-dihydroxy-4-(hydroxymethyl)tetrahydro-2-furanyl]-beta-d-glucopyranoside	$C_{18}H_{34}O_{12}$	0.869
51	7.18	152.0720	153.0790	122.03, **152.02**	Dopamine	$C_8H_{11}NO_2$	0.887
52	7.87	311.1500		183.00, 201.10, 223.16, 292.19, **311.21**	Pyrenophorol	$C_{16}H_{24}O_6$	0.971
53	7.92	[M+FA-H]- 720.4330	675.4350	119.03, 179.05, 235.07, 277.21, 463.31, **675.33**	3-[(2-Acetamido-2-deoxyhexopyranosyl)oxy]-16-hydroxyolean-12-en-28-oic acid	$C_{38}H_{61}NO_9$	0.744
54	8.41	277.2400	277.2250	71.02, 133.05, 196.05, **277.21**	Linolenic acid	$C_{18}H_{30}O_2$	0.916
55	8.46	408.3200	409.570	408.3200	N-[1-(diethylamino)-3-morpholin-4-ylpropan-2-yl]-2,2-diphenylacetamide	$C_{25}H_{35}N_3O_2$	0.986
56	8.53	477.4300		239.14, 439.34, **474.24**	isorhamnetin-3-O-glucoside	$C_{22}H_{22}O_{12}$	0.776
57	8.53	339.3276		79.95, 120.04, **163.10**, 183.00, 262.08	Behenic acid	$C_{22}H_{44}O_2$	0.924

metabolites. The justification for picking only 5 metabolites from a list of 57 tentatively identified metabolites was that only 5 metabolites out of 57 tentatively identified ones were selected based on \their binding energy being less than −6 and having no violations of the Lipinski rule, which is crucial for a medicinal compound. Furthermore, evaluations using www.swissadme.ch and https://ox-new.charite.de/protox showed that the chosen metabolites had superior ADMET characteristics compared to the others. The ligand molecules L1 (CID: 3961), losartan, L2 (CID:44208), (N-[1-(diethylamino)-3-morpholin-4-ylpropan-2-yl]-2,2-diphenylacetamide), L3 (CID:10935870), pyrenophorol, L4 (CID:73824231), Isoarthonin, L5 (CID:45359729) (2E,4E)-N-[2-(4-hydroxyphenyl)ethyl]dodeca-2,4-dienamide, and the reference drugs, Diclofenac L6 (CID:3033) (2-[2-(2,6-dichloroanilino)phenyl]acetic acid and ibuprofen L7 (CID: 3672) (2-[4-(2-methylpropyl)phenyl]propanoic acid) were retrieved from the PubChem database and generated as a three-dimensional structure using the Marvin Sketch tool. The bond errors were corrected accordingly. The energy minimization and structural conformation of the ligands were performed using the PRODRG server [22].

2.3. Selecting the target protein and predicting the binding site

The three-dimensional crystal structures of diclofenac, and ibuprofen bound to the active COX-2 cyclooxygenase site (PDB: 1PXX) were recovered from the Protein Data Bank (PDB) (http://www.pdb.org). The docking study incorporated the identification of the protein's active binding sites through an analysis of CASTP, and COACH server [23–25]. For proteins and other molecules, it provides identification and sizes for both accessible surface pockets and inaccessible interior cavities.

2.4. Analyzing molecules via docking

The docking simulation was carried out using Auto dock tools [26]. The selected ligand molecules and the standard drug were docked to

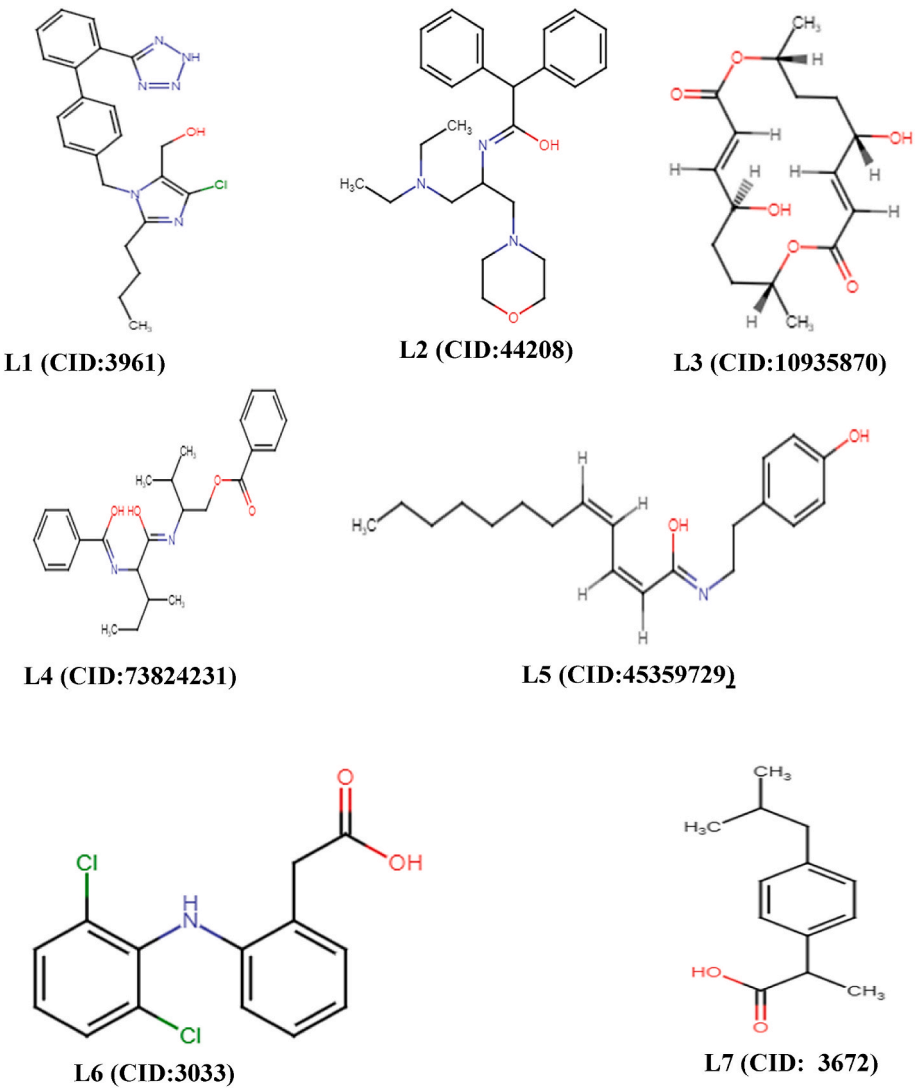

Fig. 1. The five metabolites selected from *D. batokana* as anti-inflammatory drug candidates, and the reference drugs - diclofenac and ibuprofen.

target proteins COX-2 (PDB: 1PXX) with the molecules treated as a rigid body and the ligands being flexible. All docking experiments consisted of 10 docking runs with 150 individuals and 500,000 energy evaluations using a Lamarckian Genetic Algorithm (LGA) [27]. LGA is a significantly validated algorithm for identifying the ligand-protein conformation space that strikes a balance between systematic search and computational efficiency. Moreover, the defined energy scores and population size confirm the conformational space and the best binding position of the ligand based on the desired docking runs [26]. The search was extended in a grid of 70 points per dimension and a step size of 0.375 Å centered on the binding site of the target protein. The Auto Dock results indicated the binding position and bound conformation of the active sites, as well as the estimation of its interaction. The docked conformation which had the least binding energy was selected to analyze the mode of binding. In general, the standard criterion for selecting the best docked conformation (>-5 kcal) is the lowest binding energy of the ligand, which usually correlates with the biologically relevant interactions [27,28]. The hydrogen bond and various interactions of ligand-protein complex were analyzed by the Discovery Studio 2021 Client l molecular viewer.

2.5. ADMET studies

Adsorption, Distribution, Metabolism, Excretion, and Toxicity (ADMET) analysis is crucial for figuring out the molecule's pharmacodynamic characteristics. Using a Web-based online system called SWISSADME (www.swissadme.ch/; last accessed on 18 January 2024), the ADMET properties of pharmaceuticals and natural bioactive metabolites with the most likely matches were found [29]. Ligand smiles retrieved from PubChem were submitted to SWISSADME.

2.6. Determination of toxicity

An online Web tool ProTox-II was used to andalyze and predict the toxicity of metabolites (https://ox-new.charite.de/protox; accessed on 18 January 2024).

3. Results and discussion

3.1. Evaluation of in silico anti-inflammatory activity

A study using in silico docking was conducted to determine the ability of certain metabolites to inhibit the target protein, COX-2. The findings of the in silico molecular docking analysis are shown in Table 2 and Fig. 2. The 2D and 3D interaction complex of ligands (L1, L2, L3, L4, L5, and L6) with the COX-2 receptor is shown in Fig. 2. (a) The two-dimensional interactions of the ligand with the active site, and (b) the interaction of the ligand-active site in three dimensions. The results of

Table 2
The results of in silico molecular docking of target metabolites with the COX2-receptor (1PXX).

Ligand	Interacting residues & atoms in bond (ligand - Receptor)	Interaction type	Distance	Binding Energy (kcal/mol)	Vdw_hb_ desolv_energy (kcal/mol	Inhibition constant	Ligand efficiency
L1 3961 (Losartan)	HIS214: HE2-N	H-Bond: Conventional H-Bond	1.9981	−7.59	−10.21	2.74 (μM)	0.25
	HIS388: HE2-N	H-Bond: Conventional H-Bond	2.9372				
	TYR385: O–H	H-Bond: Conventional H-Bond	2.0023				
	HIS388: HE1-N	H-Bond: Carbon H-Bond	2.8093				
	HIS207: NE2	Electrostatic: Pi-Cation	4.0298				
	HIS214: NE2	Electrostatic: Pi-Cation	4.1525				
	HIS386: NE2	Electrostatic: Pi-Cation	4.2683				
	HIS386	Hydrophobic: Pi-Pi Stacked	4.1552				
	HIS207	Hydrophobic: Pi-Pi T-shaped	4.8146				
	HIS207	Hydrophobic: Pi-Pi T-shaped	4.5214				
	HIS214	Hydrophobic: Pi-Pi T-shaped	4.9728				
	VAL447	Hydrophobic: Alkyl	5.4858				
	HIS207: Cl	Hydrophobic: Pi-Alkyl	5.4853				
	HIS386	Hydrophobic: Pi-Alkyl	4.1339				
	HIS388: Cl	Hydrophobic: Pi-Alkyl	4.2988				
L2 44208	HIS207: HE2-O	H-Bond: Conventional H-Bond	1.8711	−7.05	−9.81	6.81 (μM)	0.24
	THR212: HG1-O	H-Bond: Conventional H-Bond	2.1576				
	ASN382: HD22-O	H-Bond: Carbon H-Bond	1.7563				
	HIS207: HE1-O	H-Bond: Pi-Donor H-Bond	2.9537				
	HIS388: NE2	Electrostatic: Pi-Cation	3.2988				
	HIS388	Hydrophobic: Pi-Pi T-shaped	4.1446				
	VAL447	Hydrophobic: Alkyl	3.4573				
	LEU391	Hydrophobic: Pi-Alkyl	5.2226				
	VAL291	Hydrophobic: Pi-Alkyl	4.7869				
	VAL295	Hydrophobic: Pi-Alkyl	5.4279				
L3 10935870 (pyrenophorol)	SER530: HG-O	H-Bond: Conventional H-Bond	1.8083	−7.37	−8.16	9.28 (μM)	0.34
	TYR385: OH–H	H-Bond: Conventional H-Bond	2.0263				
	VAL349	Hydrophobic: Pi-Alkyl	4.9897				
	VAL523	Hydrophobic: Pi-Alkyl	4.6472				
	ALA527	Hydrophobic: Pi-Alkyl	4.5395				
L4 73824231 (isoarthonin)	TRP387: HN–O	H-Bond: Conventional H-Bond	2.3682	−6.26	−9.47	25.76 (μM)	0.20
	HIS388: HE2-O	H-Bond: Conventional H-Bond	2.4456				
	GLN203: OE1-H	H-Bond: Conventional H-Bond	1.8035				
	HIS386: HA-O	H-Bond: Carbon H-Bond	2.9819				
	HIS388: HD2-O	H-Bond: Carbon H-Bond	1.8031				
	HIS207: NE2-0	Electrostatic: Pi-Cation	4.5799				
	HIS207: NE2	Electrostatic: Pi-Cation	4.1616				
	HIS386	Hydrophobic: Pi-Pi Stacked	4.2540				
	HIS207	Hydrophobic: Pi-Pi T-shaped	4.8408				
	HIS207	Hydrophobic: Pi-Pi T-shaped	5.0952				
	ALA199	Hydrophobic: Alkyl	3.0412				
	VAL295	Hydrophobic: Alkyl	5.2617				
	LEU390	Hydrophobic: Alkyl	3.8297				
	LEU391	Hydrophobic: Alkyl	4.4654				

(*continued on next page*)

Table 2 (*continued*)

Ligand	Interacting residues & atoms in bond (ligand - Receptor)	Interaction type	Distance	Binding Energy (kcal/mol)	Vdw_hb_ desolv_energy (kcal/mol	Inhibition constant	Ligand efficiency
	VAL291	Hydrophobic: Pi-Alkyl	4.3369				
L5 45359729	ALA199: O–H	H-Bond: Conventional H-Bond	2.01175	−6.60	−10.16	14.54 (μM)	0.29
	TYR385: O–C	H-Bond: Carbon H-Bond	3.01483				
	TRP387: HB1	Hydrophobic: Pi-Sigma	2.62179				
	ALA202: C,O; GLN203: N	Hydrophobic: Amide-Pi Stacked	4.48377				
	TRP387: C,O; HIS388: N	Hydrophobic: Amide-Pi Stacked	4.55699				
	VAL291	Hydrophobic: Alkyl	3.47922				
	HIS207	Hydrophobic: Pi-Alkyl	5.1093				
	PHE210	Hydrophobic: Pi-Alkyl	5.38945				
	HIS386	Hydrophobic: Pi-Alkyl	5.37978				
	ALA202	Hydrophobic: Pi-Alkyl	4.3997				
	LEU390	Hydrophobic: Pi-Alkyl	5.13132				
L6 3033 (diclofenac)	SER530: HG-O	H-Bond: Conventional H-Bond	1.8083	−6.87	−8.16	9.28 (μM)	0.36
	TYR385: OH–H	H-Bond: Conventional H-Bond	2.0263				
	VAL349	Hydrophobic: Pi-Alkyl	4.9897				
	VAL523	Hydrophobic: Pi-Alkyl	4.6472				
	ALA527	Hydrophobic: Pi-Alkyl	4.5395				
L7 3672 (ibuprofen)	CYS D: 3047 (HN–N)	H-Bond: Conventional H-Bond	1.98277	−5.63	−6.68	87.28 (μM)	−0.35
	PRO D: 3154 (O–OH)	H-Bond: Conventional H-Bond	2.31436				
	GLY D: 3045 (O–H)	H- Bond: Carbon Hydrogen bond	3.15818				
	PRO D: 3153	Hydrophobic:Pi-Alkyl	4.66516				
	PRO D: 3153	Hydrophobic: Pi-Alkyl	4.37381				
	CYS D: 3041	Hydrophobic: Pi-Alkyl	4.71147				
	CYS D: 3047	Hydrophobic: Pi-Alkyl	4.55947				
	CYS D: 3047	Hydrophobic: Pi-Alkyl	5.11281				

the in silico molecular docking of the selected metabolites of *D. botakana* with the COX 2 receptor are shown in Table 2 and include information on interaction type, distance, binding energy, affinity, inhibition constant and ligand efficiency.

The accuracy of computational simulations in silico docking studies, which predict the binding affinity of a small molecule to a protein target, is dependent on a number of variables, including the nature of the interaction between the ligand and the protein. The three primary classes of interactions between the ligand and the Cox-2 receptor are hydrogen bonding, hydrophobic interactions, and electrostatic interactions, as indicated by the results shown in Fig. 2 and Table 2. The binding affinity of the ligand to the protein target is determined in large part by each of these interaction types, as previous reports have shown [30,31]. For example, the hydrophobic interactions shown in Fig. 2 and Table 2 increase the stability of the ligand-protein receptor complex by decreasing the solvent-accessible surface area of the protein-ligand interface, while hydrogen bonding is necessary for the formation of stable complexes between the ligand and the protein [32]. On the other hand, charged groups in the ligand and the protein must be recognized in order for electrostatic interactions to occur [33]. Therefore, in silico docking studies, accurately predicting the binding affinity of a small molecule to a protein target requires understanding of the significance of each interaction type.

3.1.1. Binding energy

In in silico molecular docking, the binding energy is a crucial parameter. The binding energy refers to the energy released when two molecules bond [34]. The strength of the interaction between these molecules is assessed through the binding energy. This metric is employed in molecular docking to expect the strength of interaction between a protein and a ligand. It should be noted that a lower binding energy value signifies a stronger interaction between the ligand and the protein [34]. Using in silico molecular docking enables researchers to predict the binding affinity of a potential drug candidate to a target protein, offering valuable insights for the drug discovery process. L3, L2, and L1, all had ligand binding energies to the target protein, COX-2, of −7.37, −7.05, and −7.59 kcal/mol, respectively (Table 2). All of these binding energies are less than the −6.87 kcal/mol, and −5.63 kcal/mol binding energies of the drugs used as a references, diclofenac and ibuprofen respectively. This indicates that compared to diclofenac, L1, L2, and L3 with lower binding energy values may be a better anti-inflammatory drug. However, L4 and L5 had binding energies of −6.26 and −6.60 kcal/mol, respectively which are all greater than the binding energies of the reference drugs, diclofenac and ibuprofen. This indicates that these two metabolites may be less effective as anti-inflammatory drugs compared to the standard, diclofenac.

3.1.2. Binding affinity (Vdw_hb_desolv_energy)

For in silico molecular docking, the van der Waals (vdW), hydrogen bonding (H bond), and desolvation (desolv) energies are crucial parameters. The force that attracts or repels two molecules based on their electron density is known as the vdW energy. The energy needed to break a hydrogen bond between two molecules is known as the H-bond energy. The energy needed to eliminate water molecules from the surface of a molecule is known as desolv energy. During molecular docking, these energies are used to determine the binding affinity between two molecules [35]. The degree to which two molecules, a ligand and its target (protein receptor), bind to one another is determined by their binding affinity [35]. A greater affinity for binding signifies a more robust intermolecular interaction. Table 2 shows that the complexes have binding affinities ranging from −8.0 to 10.21 kcal/mol, confirming their exceptional potential as anti-inflammatory drug candidates. With a binding affinity of −10.21 kcal/mol, L1 may be the most promising anti-inflammatory inhibitor. Losartan has the highest anti-inflammatory

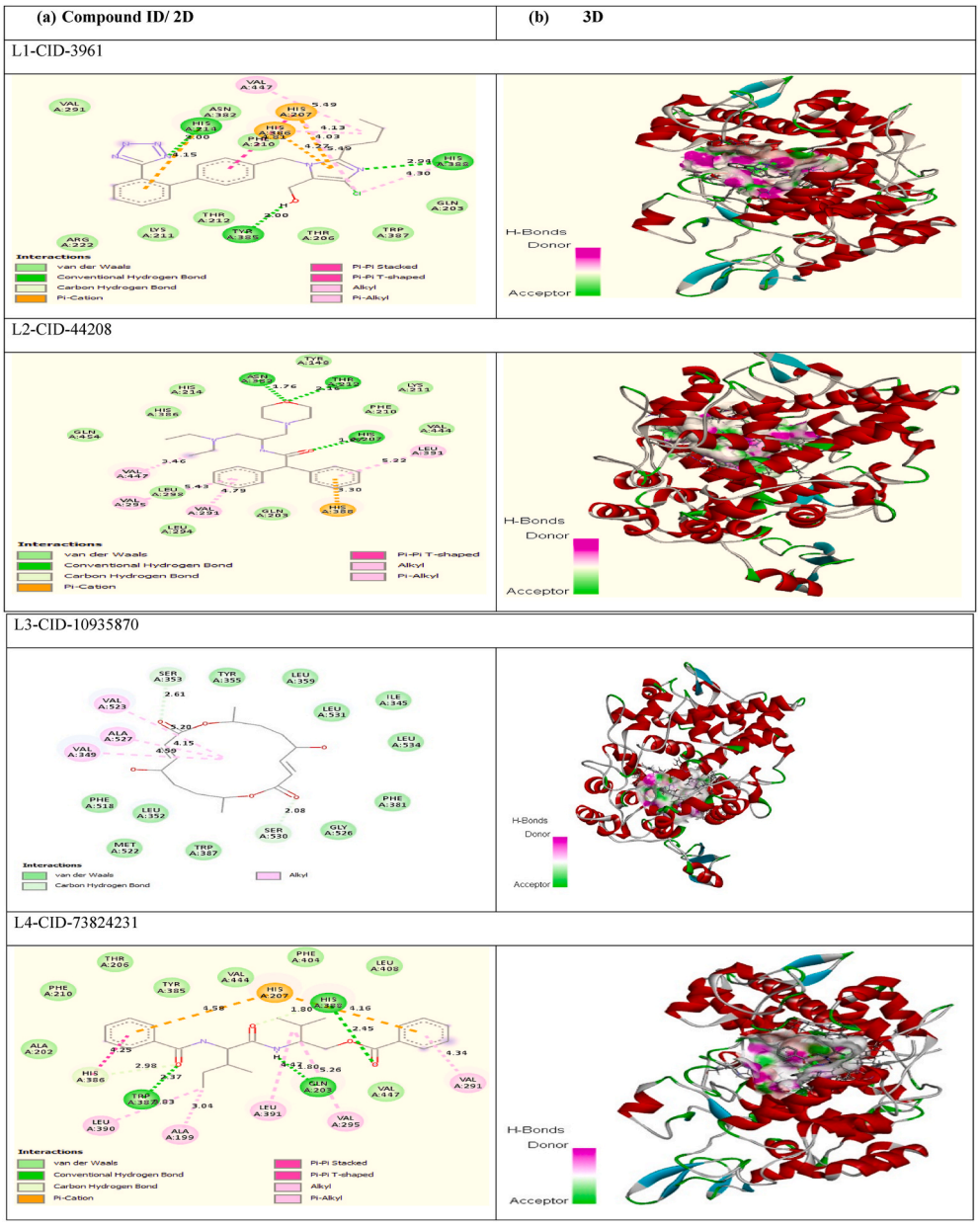

Fig. 2. Complex of 2D and 3D interactions of the compound of interest with the COX-2 receptor. (a) 2D interactions of ligand with the active site; (b) 3D interactions of ligand with the active site.

potency, followed by L5, (−10.16 kcal/mol), L4, (−9.47 kcal/mol), and L2, (−9.81 kcal/mol). Therefore, based on binding affinity, all of these *D. batokana* ligands can be better anti-inflammatory candidates than diclofenac (−8.16 kcal/mol), and ibuprofen (−6.68 (kcal/mol). L3, has the same binding affinity to that of diclofenac potency, at −8.16 kcal/mol.

3.1.3. Inhibition constant

When docked, the inhibition constant, Ki, represents the dissociation constant of the enzyme-inhibitor complex. A smaller Ki value indicates a lower possibility of dissociation, resulting in higher inhibition. It indicates the inhibitor's binding strength and is crucial in understanding drug interactions [18]. The Ki is calculated based on the basis of the concentration needed to decrease an enzyme's activity by half. A lower Ki indicates a higher binding affinity and lower dosage requirements for inhibiting the enzyme [18]. Thus, in the docking context, the Ki value is used to assess the level of interaction between the protein receptor and the ligand. A lower Ki value signifies a stronger interaction. This information can be applied to predict the effectiveness of a drug in halting the physiological activity of a protein receptor.

L1, L2 and L3 were the three metabolites with lower inhibition constants of 2.74, 3.98, and 6.81 μM, respectively (Table 2). Losartan had the lowest inhibition constant compared to diclofenac, and ibuprofen the standard anti-inflammatory drugs, at 9.28 μM and 87.28 μM respectively. This indicates that these three metabolites may be superior to diclofenac and ibuprofen as inflammation inhibitors based on inhibition constants. However, two metabolites L4 and L5 had relatively higher inhibition constants at 25.76 and 14.54 μM, respectively, compared to diclofenac (9.28 μM), but far better than ibuprofen (87.28 μM).

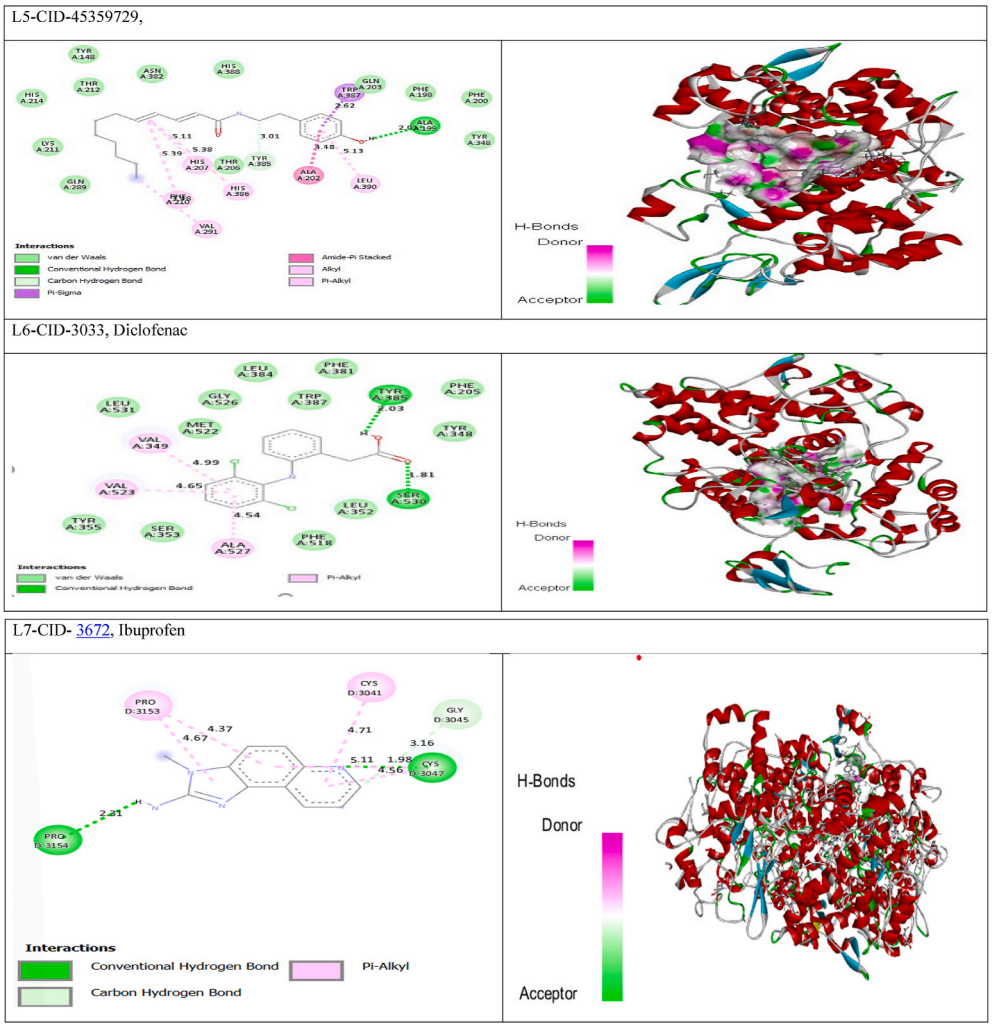

Fig. 2. (*continued*).

3.1.4. *Ligand efficiency*

Ligand efficiency indicates how effectively a ligand attaches to a target protein [36]. This efficiency is calculated by dividing the molecular weight of the ligand by its binding affinity. In the context of in silico molecular docking, ligand efficiency is a tool to evaluate the quality of the ligand-protein complex formed when the ligand binds to the protein's active site. A high ligand efficiency score indicates an efficient binding between the ligand and the protein, making the ligand a promising candidate for further optimization and drug development. Therefore, ligand efficiency plays a vital role in in silico molecular docking, aiding in the identification of ligands that are likely to effectively bind to the target protein and be developed into pharmaceuticals [36].

According to the results in Table 2, the most effective ligands are diclofenac (0.36) and ibuprofen (0.35). L3 (0.34), L5 (0.29), L1 (0.25), L2 (0.24), and L4 (0.20) have relatively lower ligand efficiencies than the two standard drugs diclofenac and ibuprofen.

3.1.5. *ADMET analysis*

A drug molecule needs to reach its target in the body at a concentration high enough and remain there in a bioactive form for the anticipated biological events to take place in order for it to be effective as a medication [37]. In the process of developing new drugs, absorption, distribution, metabolism, and excretion (ADME) are evaluated in progressively earlier stages of the discovery phase, when the number of potential compounds is high but physical sample access is restricted. A variety of quick and reliable predictive models for physicochemical properties, pharmacokinetics, drug-likeness, and medicinal chemistry friendliness are available via the new SwissADME web tool. These models include highly skilled internal techniques, such as the BOILED Egg and Bioavailability Radar. The user-friendly interface provided by the log-in-free website http://www.swissadme.ch allowed for easy and efficient input and interpretation in this study.

The physiochemical and pharmacokinetic (PK) properties of the selected *D. batokana metabolites* such as L1, L2, L3, L4 and L5 along with the reference drug, diclofenac and ibuprofen were investigated. All the selected metabolites complied with Lipinski's rule of five. Intestinal absorption is a critical precondition for assessing an oral drug's apparent efficacy. All the five metabolites in the current study showed significant GI absorption. The 57 isozymes that comprise the human cytochrome P450 family (phase I enzymes) metabolize around two-thirds of all known medications; 5 isozymes, namely 1A2, 3A4, 2C9, 2C19, and 2D6, account for 80 % of this process. The majority of these cytochrome P450 (CYPs) that regulate phase I reactions are found in the liver. The output value in this study is the likelihood of being an inhibitor or a substrate, with a range of 0 (No) to 1 (Yes). The assessment of synthetic accessibility evaluates how simple it is to synthesize a wide range of metabolites that could potentially result in a breakthrough in drug discovery. Scores are assigned using this approach, which goes from 1 (easy to make) to 10 (difficult to make). In the present study, synthetic accessibility scores for L1, (L2), L3, L4 and L5 were 3.45, 3.58, 4.90, 3.93, and 2.4 respectively, in relation to the standards, diclofenac (2.23) and

Table 3
ADMET results of the five metabolites of *D. batokana* and the reference drugs; diclofenac and ibuprofen.

Admet Properties	Metabolites					Reference drug	
	L1	L2	L3	L4	L5	L6 diclofenac	L7 ibuprofen
Size (MW) g/mol	422.91	409.56	312.36	424.53	315.45	296.15	206.28
Lipophilicity XLOGP3	4.29	3.33	1.43	5.21	5.75	4.40	3.50
Solubility Log S (ESOL)	−5.18	−4.05	−2.68	−5.18	−2.89	−4.65	−3.36
Saturation Fraction Csp3	0.27	0.48	0.62	0.40	0.45	0.07	0.46
Flexibility (Num. rotatable bonds)	8	11	0	13	12	4	4
Num. H-bond acceptors	5	4	6	4	2	2	2
Num. H-bond donors	2	1	2	2	2	2	1
Molar refractivity	117.11	125.26	80.86	121.31	97.98	77.55	62.18
Polarity TPSA ($Å^2$)	92.51	44.81	93.06	84.50	49.33	49.33	37.30
Lipophilicity							
XLOGP3	4.29	3.33	1.43	5.21	5.75	4.40	3.50
iLOGP	2.59	3.97	2.52	3.80	3.86	1.98	2.7
WLOGP	4.11	2.60	1.26	3.83	4.52	4.36	3.07
MLOGP	3.36	2.31	0.95	3.49	3.65	3.84	3.13
SILICOS-IT	4.94	3.96	0.48	4.50	5.23	3.74	
Lipophilicity average	3.86	3.23	1.33	4.16	4.60	3.66	3.00
Druglikeness							
Lipinski	Yes; 0 violation	Yes; 0 violation	Yes; 0 violation	Yes; 0 violation	Yes; 0 violation	Yes; 0 violation	Yes; 0 violation
Ghose	Yes	Yes	Yes	Yes	Yes	Yes	Yes
Veber	Yes	No; 1 violation: Rotors>10	Yes	No; 1 violation: Rotors>10	No; 1 violation: Rotors>10	Yes	Yes
Egan	Yes	Yes	Yes	Yes	Yes	Yes	Yes
Muegge	Yes	Yes	Yes	No; 1 violation: XLOGP3>5	No; 1 violation: XLOGP3>5	Yes	Yes
Bioavailability score	0.56	0.55	0.55	0.55	0.55	0.85	0.85
Pharmacokinetics							
Gastrointestinal (GI) absorption	High	High	High	High	High	High	High
Blood brain barrier (BBB) permeability	No	Yes	No	No	Yes	Yes	Yes
P-gp substrate	Yes	No		Yes	No	No	No
CYP1A2 inhibitor	No	No	No	No	Yes	Yes	No
CYP2C19 inhibitor	Yes	No	No	Yes	Yes	Yes	No
CYP2C9 inhibitor	Yes	No	No	Yes	Yes	Yes	No
CYP2D6 inhibitor	Yes	Yes	No	Yes	No	Yes	No
CYP3A4 inhibitor	Yes	Yes	No	Yes	Yes	No	No
Log Kp (skin permeation) cm/s	−5.83	−6.43	−7.19	−5.19	−4.14	−4.98	−5.07
Pan assay interference compounds (PAINS)	0	0	0	0	0	0	0
Brenk	0		1	0	2 alerts: michael_acceptor_1, polyene	0	0
Leadlikeness	No; 3 violations: MW>350, Rotors>7, XLOGP3>3.5	No; 2 violations: MW>350, Rotors>7	Yes	No; 3 violations: MW>350, Rotors>7, XLOGP3>3.5	No; 2 violations: Rotors>7, XLOGP3>3.5	No; 1 violation: XLOGP3>3.5	No; 1 violation: MW>250
Synthetic accessibility	3.45	3.58	4.90	3.93	2.94	2.23	1.92

ibuprofen (1.92). Table 3 presents the findings from the ADME analysis.

The bioavailability radar for the relevant metabolites is shown in Fig. 3. For an instant evaluation of a drug's likeness, the bioavailability radar is presented. Lipophilicity, size, polarity, solubility, flexibility, and saturation are the six physicochemical properties taken into account (Table 3). The optimal range for each property is represented by the pink area (Fig. 3) [37]. These properties include: polarity (TPSA, 20–130 Å2), size (MW, 150–500 g/mol), solubility (log S, no more than 6), saturation (fraction of carbons in the sp^3 hybridization, no less than 0.25), and flexibility (no more than 9 rotatable bonds). It is obvious that L4 and L2 will not be bioavailable orally in this regard. This is due to the fact that isoarthonin is too flexible and N-[1-(diethylamino)-3-morpholin-4-ylpropan-2-yl]-2,2-diphenylacetamide is not sufficiently saturated. Losartan and pyrenophorol are therefore predicted to be bioavailable and suitable drug candidates.

A physicochemical range on each axis, represented as a pink area in Fig. 3 and Table 3, was defined by descriptors taken from Ritchie et al. (2011) and Lovering et al. (2009) [38,39]. A molecule must fall entirely within this range on the radar plot to be classified as drug-like. Compared to L2 and L4, whose radar plots partially fall outside the pink area, the metabolites losartan and pyrenophorol fall entirely inside the pink area, making them the best candidates for drug development. Concerning this parameter, the reference drug Diclofenac is not a good medicine because part of its radar plot is outside of the pink area. However, ibuprofen is a good medicine because the whole of its radar plot is inside the pink area.

3.1.6. Toxicity analysis

ProTox-II is a valuable tool in the drug design and development process since it can predict the toxicities of small compounds. Several criteria, including hepatotoxicity, LD50, predicted toxicity class, cytotoxicity, mutagenicity, immunotoxicity, and carcinogenicity were taken into account for the toxicity analysis in the current study. The following criteria were used to classify the toxicity levels into various groups. Class I: lethal if ingested (LD50 $\leq$ 5 mg/kg); Class II: lethal if ingested (5 mg/kg $<$ LD50 $\leq$ 50 mg/kg); Class III: toxic if ingested (50 mg/kg $<$ LD50 $\leq$

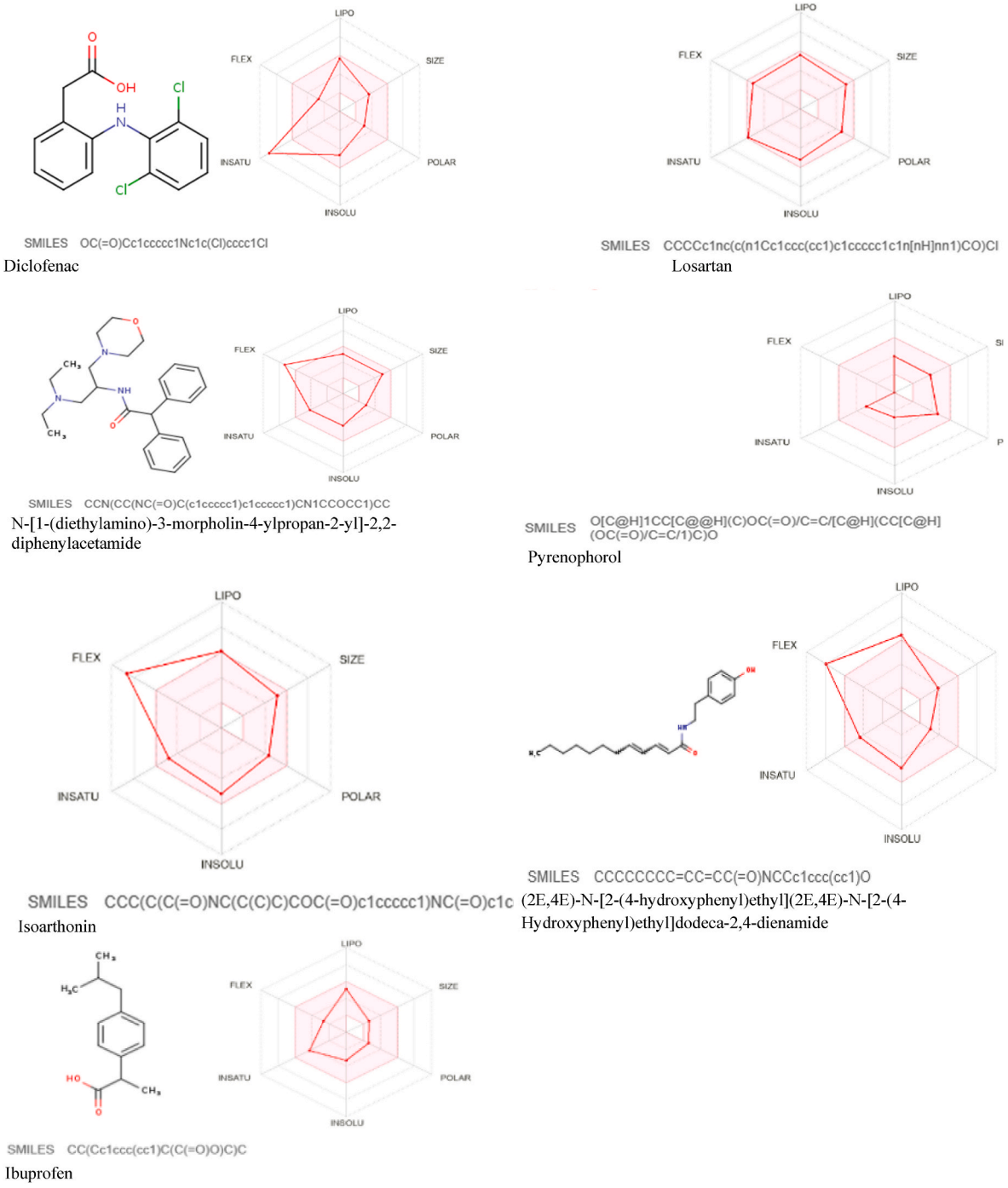

Fig. 3. The Bioavailability Radar for the relevant metabolites and the reference drugs, diclofenac and ibuprofen.

300 mg/kg); Class IV: detrimental if ingested (300 mg/kg < LD50 ≤ 2000 mg/kg); Class V: potentially harmful if ingested (2000 mg/kg < LD50 ≤ 5000 mg/kg); and Class VI: non-toxic [29].

A number of toxicity endpoints, such as carcinogenicity, hepatotoxicity, immunotoxicity, mutagenicity, and cytotoxicity were assessed using ProTox-II. Predictive models are constructed utilizing data from in vivo tests (hepatotoxicity, carcinogenicity) as well as in vitro tests (Tox21 tests, immunotoxicity assays, Ames bacterial mutation studies, and hepG2 cytotoxicity assays). In the present study, selected bioactive metabolites L2, L3, and L4 were inactive for immunotoxicity, hepatotoxicity, cytotoxicity, carcinogenicity, and mutagenicity. However, losartan was active for immunotoxicity, cytotoxicity, and mutagenicity. Metabolite L5 was only active for immunotoxicity. This was in relation to the reference drugs, diclofenac and ibuprofen, which were both active for hepatotoxicity and immunotoxicity. Table 4 displays the expected toxicity analysis probabilities.

4. Conclusions

In silico investigation of selected metabolites of *D. batokana* targeting potential drug candidates for anti-inflammatory drugs such as COX-2 inhibitors has produced promising results. The analysis yielded favorable binding energies, affinities, inhibition constants and ligand efficiencies when docking to COX-2 (1PXX) and compared them to the reference ligand, diclofenac. Similarly, the ADMET analysis data for the selected ligands appear promising compared to those of diclofenac and

Table 4
Toxicity analysis of phytocompounds from *D. batokana* and the reference drugs, diclofenac and ibuprofen.

Metabolites	Predicted LD50	Predicted toxicity class	Hepatotoxicity (prediction/probability)	Carcinogenicity (prediction/probability)	Mutagenicity (prediction/probability)	Immunotoxicity (prediction/probability)	Cytotoxicity (prediction/probability)
L1	300 mg/kg	3	Inactive/0.63	Inactive/0.58	Active/0.54	Active/0.80	Inactive/0.55
L2	370 mg/kg	4	Inactive/0.89	Inactive/0.62	Inactive/0.74	Inactive/0.91	Inactive/0.83
L3	5000 mg/kg	5	Inactive/0.76	Inactive/0.67	Inactive/0.83	Inactive/0.54	Inactive/0.57
L4	2250 mg/kg	5	Inactive/0.71	Inactive/0.61	Inactive/0.76	Inactive/0.99	Inactive/0.63
L5	1250 mg/kg	4	Inactive/0.82	Inactive/0.61	Inactive/0.76	Active/0.91	Inactive/0.83
Diclofenac (L6)	1190 mg/kg	4	Active/0.69	Inactive/0.62	Inactive/0.97	Active/0.96	Inactive/0.93
Ibuprofen (L7)	1190 mg/kg	4	Active/0.69	Inactive/0.62	Inactive/0.97	Active/0.96	Inactive/0.93

ibuprofen. The results suggest that L3 (pyrenophorol), L2 (N-[1-(diethylamino)-3-morpholin-4-ylpropan-2-yl]-2,2-diphenylacetamide), L1 (losartan), L4 (isoarthonin) and (2E,4E)-N-[2-(4-hydroxyphenyl)ethyl] dodeca-2,4-dienamide could serve as excellent anti-inflammatory drug candidates, potentially acting as COX-2 cyclooxygenase inhibitors. These compounds exhibit inhibition capacities similar to those of the prescription drugs, diclofenac and ibuprofen. In particular, L3 and L5 show the highest diclofenac and ibuprofen-like properties in terms of ligand efficiency. In terms of inhibition constants, L3, L2 and L1 are indicated as potentially more effective medications to inhibit COX-2 cyclooxygenase activation. Furthermore, binding energies and affinities demonstrate that L3, L2, L1, L4 and L5 could be valuable as anti-inflammatory drug candidates, supporting the traditional uses of the studied plant, *D. batokana*. Furthermore, bioavailability radar and physicochemical properties predict L1, L3 and L5 bioavailable and suitable drug candidates. Finally, ADME analysis show that L1 and L3 would be better drugs comparable to ibuprofen, than diclofenac. In the same vein, toxicity analysis show that L2, L3, and L4 are less toxic compared to both diclofenac and ibuprofen. In summary, L1 (losartan), L3 (pyrenophorol), and L5 (2E,4E)-N-[2-(4-hydroxyphenyl)ethyl] dodeca-2,4-dienamide) are excellent drug candidates for future drug development as COX-2 inhibitor. In silico and ADMET analysis, shows that the five metabolites could be used as anti-inflammatory drugs comparable to the standard drugs, diclofenac and ibuprofen.

CRediT authorship contribution statement

Bitwell Chibuye: Writing – review & editing, Writing – original draft, Software, Resources, Project administration, Methodology, Investigation, Funding acquisition, Formal analysis, Data curation, Conceptualization. **Indra Sen Singh:** Writing – review & editing, Visualization, Validation, Supervision, Software, Resources, Methodology, Funding acquisition. **Luke Chimuka:** Validation, Supervision, Resources, Methodology. **Kenneth Kakoma Maseka:** Supervision.

Declaration of competing interest

The authors declare that they have no known competing financial interests or personal relationships that could have appeared to influence the work reported in this paper.

Data availability

Data will be made available on request.

Acknowledgments

The authors wholeheartedly acknowledge the support rendered by the Ministry of Education of the Republic of Zambia, Copperbelt University – Africa Centre of Excellence in Sustainable Mining (CBU – ACESM), University of the Witwatersrand, and Mukuba University, without which this study would not have been achievable. No role was played by these institutions in study design; in the collection, analysis and interpretation of data; in the writing of the report; and in the decision to submit the article for publication.

References

[1] N.C. Walsh, T.N. Crotti, S.R. Goldring, E.M. Gravallese, Rheumatic diseases: the effects of inflammation on bone, Immunol. Rev. 208 (1) (2005) 228–251, https://doi.org/10.1111/j.0105-2896.2005.00338.x.
[2] M. Ondua, E.M. Njoya, M.A. Abdalla, L.J. McGaw, Anti-inflammatory and antioxidant properties of leaf extracts of eleven South African medicinal plants used traditionally to treat inflammation, J. Ethnopharmacol. 234 (2019) 1–25, https://doi.org/10.1016/j.jep.2018.12.030.
[3] A. Talevi, Computer-aided drug discovery and design: recent advances and future prospects, Methods Mol. Biol. 2714 (2024) 1–20, https://doi.org/10.1007/978-1-0716-3441-7_1.
[4] J.M. Walker, Drug Design and Discovery: Methods and Protocols, Humana Press, New York, 2011.
[5] Z.A. Radi, Introduction: discovery of cyclooxygenases and historical perspective, in: Comparative Pathophysiology and Toxicology of Cyclooxygenases, 2012, https://doi.org/10.1002/9781118351918.ch.
[6] K.Y.M. Garcia, M.T.J. Quimque, G. Primahana, A. Ratzenböck, M.J.B. Cano, J.F. A. Llaguno, H.M. Dahse, C. Phukhamsakda, F. Surup, M. Stadler, A.P.G. Macabeo, COX inhibitory and cytotoxic naphthoketal-bearing polyketides from Sparticola junci, Int. J. Mol. Sci. 22 (2021) 1–13, https://doi.org/10.3390/ijms222212379.
[7] H.A.S. Murad, T.M.A. Alqurashi, M.A. Hussien, Interactions of selected cardiovascular active natural compounds with CXCR4 and CXCR7 receptors: a molecular docking, molecular dynamics, and pharmacokinetic/toxicity prediction study, BMC Complement Med Ther 22 (35) (2022) 1–22, https://doi.org/10.1186/s12906-021-03488-8.
[8] S. Johari, A. Sharma, S. Sinha, A. Das, Integrating pharmacophore mapping, virtual screening, density functional theory, molecular simulation towards the discovery of novel apolipoprotein (apoE ε4) inhibitors, Comput. Biol. Chem. 79 (2019) 83–90, https://doi.org/10.1016/j.compbiolchem.2018.12.013.
[9] A.M. Alfayomy, S.A. Abdel-Aziz, A.A. Marzouk, M.S.A. Shaykoon, A. Narumi, H. Konno, S.M. Abou-Seri, F.A.F. Ragab, Design and synthesis of pyrimidine-5-carbonitrile hybrids as COX-2 inhibitors: anti-inflammatory activity, ulcerogenic liability, histopathological and docking studies, Bioorg. Chem. 108 (2021), https://doi.org/10.1016/j.bioorg.2020.104555.
[10] R.A.A. Al-Shuaeeb, A.A. Yassin, M.A.A. Ibrahim, H.R. Abd El-Mageed, M. A. Ghandour, M.M. Khalil, Computer-based identification of olive oil components as a potential inhibitor of neirisaral adhesion a regulatory protein, J. Biomol. Struct. Dyn. 41 (5) (2023) 1553–1560, https://doi.org/10.1080/07391102.2021.2022535.
[11] F. das Chagas Pereira de Andrade, A.N. Mendes, Computational analysis of eugenol inhibitory activity in lipoxygenase and cyclooxygenase pathways, Sci. Rep. 10 (1) (2020) 1–14, https://doi.org/10.1038/s41598-020-73203-z.
[12] S. Chandra, S. Bhattacharya, Mikania scandens flower extract, J. Adv. Pharm. Educ. Res. 2 (2012) 25–31, https://doi.org/10.4103/2231-4040.90883.
[13] B. Chibuye, I. Sen Singh, L. Chimuka, K. Maseka, Phytochemical and LCMS/MS screening, total phenolic and flavonoid content and antioxidant activity of the leaves of Diospyros batokana (Ebenaceae), Sys. Rev. Pharm. 14 (2) (2023) 105–112, https://doi.org/10.31858/0975-8453.14.2.
[14] N.N. Wang, J. Dong, Y.H. Deng, M.F. Zhu, M. Wen, Z.J. Yao, A.P. Lu, J.B. Wang, D. S. Cao, ADME properties evaluation in drug discovery: prediction of caco-2 cell permeability using a combination of NSGA-II and boosting, J. Chem. Inf. Model. 56 (2016) 763–773, https://doi.org/10.1021/acs.jcim.5b00642.
[15] N.N. Wang, C. Huang, J. Dong, Z.J. Yao, M.F. Zhu, Z.K. Deng, B. Lv, A.P. Lu, A. F. Chen, D.S. Cao, Predicting human intestinal absorption with modified random

forest approach: a comprehensive evaluation of molecular representation, unbalanced data, and applicability domain issues, RSC Adv. 7 (31) (2017) 19007–19018, https://doi.org/10.1039/C6RA28442F.
[16] L. Tao, P. Zhang, C. Qin, S.Y. Chen, C. Zhang, Z. Chen, F. Zhu, S.Y. Yang, Y.Q. Wei, Y.Z. Chen, Recent progresses in the exploration of machine learning methods as in-silico ADME prediction tools, Adv. Drug Deliv. Rev. 86 (2015) 83–100, https://doi.org/10.1016/j.addr.2015.03.014.
[17] T. Hou, Editorial, Adv. Drug Deliv. Rev. 86 (1) (2015), https://doi.org/10.1016/j.addr.2015.06.006.
[18] A. Madeswaran, M. Umamaheswari, K. Asokkumar, T. Sivashanmugam, V. Subhadradevi, P. Jagannath, Docking studies: in silico lipoxygenase inhibitory activity of some commercially available flavonoids, Bangladesh J. Pharmacol. 6 (2011) 133–138, https://doi.org/10.3329/bjp.v6i2.9408.
[19] B. Chibuye, I. Sen Singh, L. Chimuka, K.K. Maseka, Phytochemical profiling and bioactivity study of Adenia panduriformis in Zambia using UHPLC-MS/MS-MZmine3, GNPS, and METLIN Gen2, Sci Afr 24 (2024) 2–16, https://doi.org/10.1016/j.sciaf.2024.e02151.
[20] R. Schmid, S. Heuckeroth, A. Korf, A. Smirnov, O. Myers, T.S. Dyrlund, R. Bushuiev, K.J. Murray, N. Hoffmann, M. Lu, A. Sarvepalli, Z. Zhang, M. Fleischauer, K. Dührkop, M. Wesner, S.J. Hoogstra, E. Rudt, O. Mokshyna, C. Brungs, K. Ponomarov, L. Mutabdžija, T. Damiani, C.J. Pudney, M. Earll, P. O. Helmer, T.R. Fallon, T. Schulze, A. Rivas-Ubach, A. Bilbao, H. Richter, L. F. Nothias, M. Wang, M. Orešič, J.K. Weng, S. Böcker, A. Jeibmann, H. Hayen, U. Karst, P.C. Dorrestein, D. Petras, X. Du, T. Pluskal, Integrative analysis of multimodal mass spectrometry data in MZmine 3, Nat. Biotechnol. 41 (2023) 447–449, https://doi.org/10.1038/s41587-023-01690-2.
[21] T. Pluskal, S. Castillo, A. Villar-Briones, M. Orešič, MZmine 2: modular framework for processing, visualizing, and analyzing mass spectrometry-based molecular profile data, BMC Bioinf. 11 (1) (2010) 1–11, https://doi.org/10.1186/1471-2105-11-395.
[22] A.W. Schüttelkopf, D.M.F. Van Aalten, PRODRG: a tool for high-throughput crystallography of protein-ligand complexes, Acta Crystallogr D Biol Crystallogr 60 (2004) 1355, https://doi.org/10.1107/S0907444904011679, 1353.
[23] J. Dundas, Z. Ouyang, J. Tseng, A. Binkowski, Y. Turpaz, J. Liang, CASTp: computed atlas of surface topography of proteins with structural and topographical mapping of functionally annotated residues, Nucleic Acids Res. 34 (2006) 116–118, https://doi.org/10.1093/nar/gkl282.
[24] J. Yang, A. Roy, Y. Zhang, BioLiP: a semi-manually curated database for biologically relevant ligand-protein interactions, Nucleic Acids Res. 41 (2013) 1096–1103, https://doi.org/10.1093/nar/gks966.
[25] J. Yang, A. Roy, Y. Zhang, Protein-ligand binding site recognition using complementary binding-specific substructure comparison and sequence profile alignment, Bioinformatics 29 (20) (2013) 2588–2595, https://doi.org/10.1093/bioinformatics/btt447.
[26] G.M. Morris, H. Ruth, W. Lindstrom, M.F. Sanner, R.K. Belew, D.S. Goodsell, A. J. Olson, Software news and updates AutoDock4 and AutoDockTools4: automated docking with selective receptor flexibility, J. Comput. Chem. 30 (16) (2009) 2785–2791, https://doi.org/10.1002/jcc.21256.
[27] R. Huey, G.M. Morris, A.J. Olson, D.S. Goodsell, A semiempirical free energy force field with charge-based desolvation, J. Comput. Chem. 28 (2007) 1145–1152, https://doi.org/10.1002/jcc.20634.
[28] A. Stalin, P. Saravana Kumar, B. Senthamarai Kannan, R. Saravanan, S. Ignacimuthu, Q. Zou, Potential inhibition of SARS-CoV-2 infection and its mutation with the novel geldanamycin analogue: ignaciomycin, Arab. J. Chem. 17 (2) (2024) 1–16, https://doi.org/10.1016/j.arabjc.2023.105493.
[29] A. Ali, G.J. Mir, A. Ayaz, I. Maqbool, S.B. Ahmad, S. Mushtaq, A. Khan, T.M. Mir, M.U. Rehman, In silico analysis and molecular docking studies of natural compounds of Withania somnifera against bovine NLRP9, J. Mol. Model. 29 (171) (2023) 1–20, https://doi.org/10.1007/s00894-023-05570-z.
[30] M. Schapira, R.F. de Freitas, Systematic analysis of atomic protein–ligand interactions in the PDB, Acta Crystallogr A Found Adv 74 (2018), https://doi.org/10.1107/s0108767318095661.
[31] R. Ferreira De Freitas, M. Schapira, A systematic analysis of atomic protein-ligand interactions in the PDB, Medchemcomm 8 (10) (2017) 1970–1981, https://doi.org/10.1039/c7md00381a.
[32] L.T. Cheng, Z. Wang, P. Setny, J. Dzubiella, B. Li, J.A. McCammon, Interfaces and hydrophobic interactions in receptor-ligand systems: a level-set variational implicit solvent approach, J. Chem. Phys. 131 (14) (2009) 1–10, https://doi.org/10.1063/1.3242274.
[33] X. Du, Y. Li, Y.L. Xia, S.M. Ai, J. Liang, P. Sang, X.L. Ji, S.Q. Liu, Insights into protein–ligand interactions: mechanisms, models, and methods, Int. J. Mol. Sci. 17 (2) (2016) 1–34, https://doi.org/10.3390/ijms17020144.
[34] M.K. Abdel-Hamid, A. McCluskey, In Silico docking, molecular dynamics and binding energy insights into the bolinaquinone-clathrin terminal domain binding site, Molecules 19 (2014) 6609–6622, https://doi.org/10.3390/molecules19056609.
[35] I.A. Shaikh, U.M. Muddapur, C. Krithika, S. Badiger, M. Kulkarni, M.H. Mahnashi, S.A. Alshamrani, M.A. Huneif, S.S. More, A.A. Khan, S.M. Shakeel Iqubal, In silico molecular docking and simulation studies of protein HBx involved in the pathogenesis of hepatitis B virus-HBV, Molecules 27 (2022) 1–12, https://doi.org/10.3390/molecules27051513.
[36] R. Dhaniaputri, H. Suwono, M. Amin, B. Lukiati, Introduction to plant metabolism, secondary metabolites biosynthetic pathway, and in-silico molecular docking for determination of plant medicinal compounds: an overview, in: Proceedings of the 7th International Conference on Biological Science (ICBS 2021), 2022, pp. 2468–5747, https://doi.org/10.2991/absr.k.220406.053.
[37] A. Daina, O. Michielin, V. Zoete, SwissADME: a free web tool to evaluate pharmacokinetics, drug-likeness and medicinal chemistry friendliness of small molecules, Sci. Rep. 7 (2017) 42717, https://doi.org/10.1038/srep42717.
[38] F. Lovering, J. Bikker, C. Humblet, Escape from flatland: increasing saturation as an approach to improving clinical success, J. Med. Chem. 52 (21) (2009) 6752–6756, https://doi.org/10.1021/jm901241e.
[39] T.J. Ritchie, P. Ertl, R. Lewis, The graphical representation of ADME-related molecule properties for medicinal chemists, Drug Discov. Today 16 (1–2) (2011) 65–72, https://doi.org/10.1016/j.drudis.2010.11.002.